

Improved methodology for computing coastal upwelling indices from satellite data

A. N. Serebrennikov

Institute of Natural and Technical Systems, Russian Academy of Sciences, Sevastopol, Russia

Abstract—The article discusses an improved methodology for determining coastal upwelling indices from satellite maps of sea surface temperature and near-surface wind. The main difference of this technique is the determination of upwelling parameters by monthly climatic masks. The algorithm for choosing monthly climate masks is considered in detail. The substantiation of the choice of the region remote from upwelling waters in the open sea is given for calculating the thermal upwelling index and its modifications. In addition to the generally accepted upwelling indices (thermal and Ekman), new indices have been introduced: cumulative and apparent upwelling power, allowing to take into account the upwelling surface area. The technique is considered on the example of the Canary Upwelling. This technique allows you to determine the boundaries of upwelling in each climate month, and therefore, more accurately calculate its indices and environmental parameters located in the upwelling region (surface wind, sea level, geostrophic current, etc.)

Index Terms—Upwelling, upwelling index, upwelling identification.

I. INTRODUCTION

Coastal upwelling is formed in the presence of a favorable alongshore wind component. The condition for its occurrence in the Northern Hemisphere is the direction of the wind component from north to south when the coast is on the left. The causes of upwelling and the methods for calculating its indices are well studied [1], [2], [3], [4], [5], [6], [7], [8]. The size of the upwelling zone depends on various factors, including wind characteristics (speed, direction, duration), type of coastline, bottom topography, interaction with surrounding waters. In coastal areas, denser cold waters that have risen to the surface create a horizontal gradient in density and temperature (upwelling front), which determines the configuration of the upwelling zone. Several authors have studied this phenomenon from different sides [9], [10], [11], [12], [13], [14], [15], [16], [17], [18], [19], [20], [21], [22]. In the paper [8], [23], an improved method was proposed for calculating the upwelling index of coastal areas using sea surface temperature (SST) images. This method is based on the use of the fuzzy c-means algorithm to find areas with uniform pixels in order to further identify the region with upwelling waters. In this paper, we propose an improved upwelling extraction technique based on the construction of monthly climatic masks within which its parameters are calculated. Thereby, they are maximally removed from the calculation of the upwelling characteristics of the region with extra-upwelling waters. During the study,

interannual dispersions of SST were constructed for each average climatic month, according to which it can be seen that the maximum interannual temperature fluctuations occur inside the climate masks. The idea of this work is to calculate the monthly average upwelling characteristics only in areas limited in area where significant temperature manifestations of upwelling were observed. Monthly temperature fields for the period 1985–2017 (climatic norms for a month) are characterized by pronounced gradients in contrast to daily and monthly maps. In these fields, one can distinguish climatic regions (masks) that will limit upwelling zones. An improved technique is considered on the example of the Canary Upwelling. During the work, daily SST maps with a spatial resolution of 0.05° in latitude and longitude for a 33-year period (from 1985 to 2017), published on the CMEMS (Copernicus Marine Environment Monitoring Service) website, and daily vector drive maps were analyzed winds for a 30-year period (from 1988 to 2017), published on the NCEP (National Centers for Environmental Prediction) website.

II. METHODOLOGY FOR THE DETERMINATION OF CLIMATIC UPWELLING MASKS

The main idea of the algorithm for finding upwelling is that the fronts in temperature images are usually thin bands separating regions of an almost constant temperature [24]. Based on this, the upwelling boundary can be found by its maximum temperature gradient. Let us determine the maximum temperature gradients for all geographical latitudes of the studied region of each climatic month. For visual control, it is proposed to calculate the monthly climatic thermal upwelling index (TUI). To calculate the TUI, it is necessary to subtract from the SST of the proposed upwelling zone the average temperature values obtained in the remote (offshore) zone from the upwelling for all latitudes of the studied area. The disadvantage of this method is the subjective choice of a remote zone. In a fairly large number of works, the authors choose the beginning of this zone from 400 to 1500 km from the coast [25]. Research data showed that the farther the offshore zone is from the coast, the more TUI is obtained. For clarity, we plotted sections of temperature fields with a resolution of 0.05 for all climatic months, both within the latitudinal limits of the proposed upwelling zone and outside it. Longitude distance was chosen 32, starting from the open ocean and ending with the coastline. The temperature values on the graph are averaged within a single-degree grid in latitude and longitude. Section plots made for the Canary

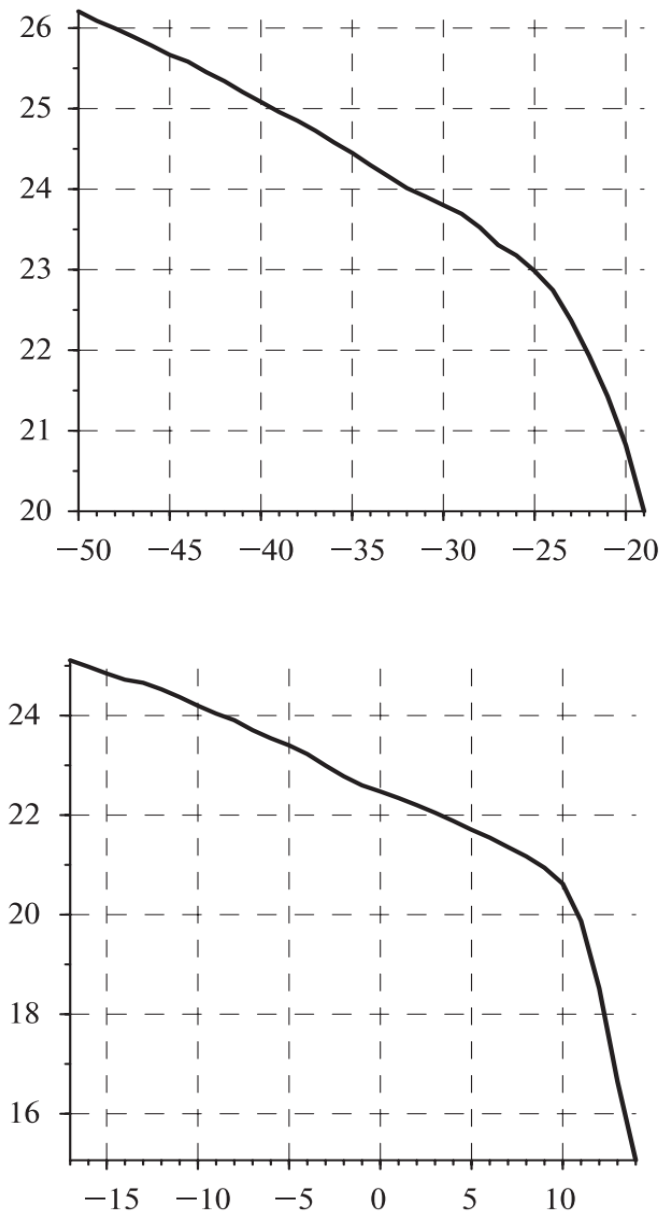


Fig. 1: Sections of monthly average SST fields in degrees Celsius for the period 1985-2017 for June at 21N for canary upwelling (above) and for April at 26S for bengel upwelling (bottom).

Upwelling at 21N in the climatic June and for the Bengel upwelling at 26°S in climatic April, are shown in fig. 1. East of 25°W for the Canary upwelling, the surface water temperature decreases noticeably more than in the other almost linear sections of the graphs. Thus, it can be assumed that 25°W and 10°E for these upwells in these reference latitudes and in given months are the points of start of the upwelling zone. We choose the offshore zone for calculating TUI with a width of 2 degrees, west of the beginning of the upwelling zone by 1 degree. At other latitudes, we will choose the offshore zone at the same distance from the coast as at the reference latitude.

For all coastal wind upwelling, we will choose the offshore zone in this way.

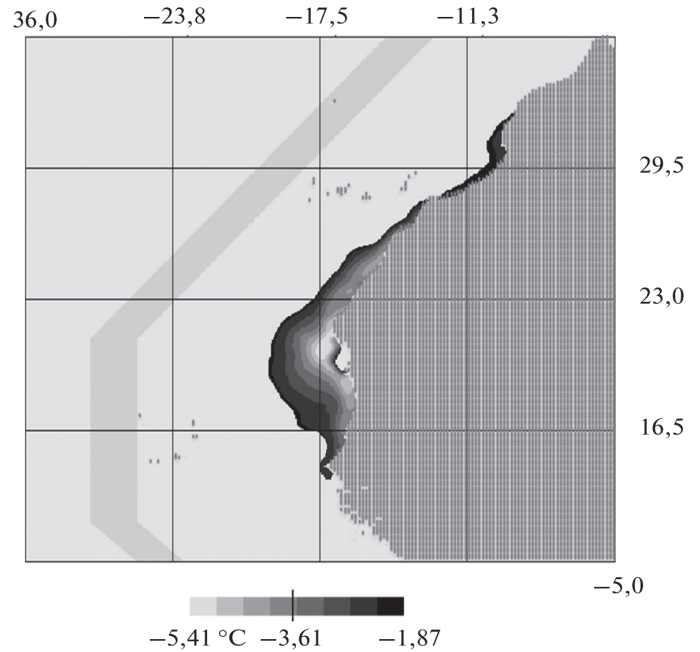


Fig. 2: Canary Upwelling. The longterm average TUI value in May for the period 1985-2017. The gray broken line shows the offshore area for calculating TUI.

The almost linear rise in the temperature of the surface of the water at the latitudes of upwelling is explained by the constant, on a climatic scale, deposition of cold upwelling waters. If you choose a rectangular offshore zone without taking into account the configuration of the coast, the distance from individual sections of the coastline to the offshore zone can vary up to 10. To minimize the error, it is proposed to choose an offshore zone configuration in which the distance to the coast will be approximately the same (Fig. 2). Next, it is necessary to identify the upwelling boundaries by the maximum temperature gradient. According to satellite data, they cannot be determined, since the maximum gradient invariably appears near the coastline itself, which does not allow us to build a mask due to the practically absent upwelling zone. However, if you limit the search for the maximum gradient by longitude and search for it at a certain (reference) latitude and in a given (reference) month, it is possible to choose the option in which the cold water will be cut off from upwelling waters and the upwelling area will be maximum. In fig. 1 shows that the maximum gradient must be sought in the range from 25°W to 20°W for the Canary Upwelling and from 10°E to 13°E for Bengel upwelling. To find the area occupied by upwelling in a certain climate month, and to determine the mask, use the method based on the following assumption. The surface temperature of the water in the upwelling zone should be lower than the temperature in the remote zone by some TL. For clarity, we compose the formula:

$$MT(m, k) < MTL_{off}(m, \phi) - T(m, \phi) \quad (1)$$

where $MT(m, k)$ is the climatic temperature for the month m and the space point k in the area of the proposed upwelling; $MTL_{off}(m, \phi)$ climatic temperature for month m and latitude ϕ in the offshore region remote from upwelling; $T(m, \phi)$ is the temperature parameter that limits the upwelling region. Moreover, the larger the T , the more limited the upwelling region and vice versa. $T(m, \phi)$ can be represented as a certain constant value, multiplied by dependent on the current month and latitude of the pair meter: $TL(m, \phi) = T_{const} \times P(m, \phi)$, where T_{const} is the temperature difference between upwelling and offshore waters in the reference month at the reference latitude; the parameter $P(m, \phi)$ is found from the ratio of the temperature $MTL_{offshore}(m, \phi)$ to the temperature $MTL_{off}(m_{fix}, \phi_{fix})$ in the given reference month (m_{fix}) at the selected reference latitude (ϕ_{fix}). Ratios are calculated for each month and for all latitudes. In order to determine T_{const} , it is necessary to find the maximum gradient in the range from 25 to 20 W. The reference month June and the reference latitude 21 were selected. Based on this criterion (separation of upwelling water from distilled water at the maximum TUI region), a temperature front with a maximum gradient was found. The temperature of this front is taken beyond the upwelling boundary at the reference point (T_{grad}). From here we get:

$$T_{const} = MTL_{off}(m, \phi) - T_{grad} \quad (2)$$

The T_{const} parameter at the reference point turned out to be 2.24C. The $T(m, \phi)$ values were in the range of 1.55-2.72 C. The smaller the T , the larger the area will be occupied by the climatic TUI, which is actually an upwelling mask. Inside the mask, we will calculate the accompanying upwelling parameters (wind, sea level, etc.). Climatic TUI was calculated for 12 months, and the monthly average for all months for the entire study period (33 years). The found upwelling parameters in the TUI regions (upwelling masks) are consistent with those described in the literature. For example, it is known that the upwelling width in the region of Cape Cap Blanc (Canary Upwelling) in January should be approximately 300 km (Cushing, 1969), which is confirmed by the obtained data.

III. RESULTS

An improved methodology for determining upwelling indices was considered using the seasonal variation of the Canary Upwelling as an example. To take into account not only the general upwelling temperature but also its area, a cumulative upwelling index (CUI) was introduced. When calculating the standard TUI value, it is necessary to calculate the average temperature in the zone of the proposed upwelling. The average TUI is independent of the upwelling area. When calculating the CUI, all negative TUI values in the expected upwelling areas are added up and the total temperature index for the entire actual upwelling area is obtained. To take into account the area of each pixel in square kilometers and its temperature, we use the following formula $CUI = \sum_{i=1}^n (tS)$ where t is the TUI index at point i in degrees Celsius; n is the number of points in the upwelling zone with a TUI of less than 0C; S point area in square kilometers, taking into

account the latitude of the terrain and spatial resolution. For the analysis and comparison of upwelling, a visible upwelling power (VUP) was proposed, which is a modification of TUI. The modification is called “visible”, since according to cosmic data, upwelling is observed by the temperature manifestation on the surface of the water. VUP shows the total temperature for the entire upwelling area. Unlike CUI in VUP, the temperature is squared to amplify large negative values (less than -1C), since they better characterize the upwelling intensity. For VUP, we obtain the following formula: $VUP = \sum_{i=1}^n (tS)$ where t -TUI at point i in degrees Celsius; n is the number of points in the upwelling zone with TUI less than 0 C; S point area in square kilometers, taking into account the latitude of the terrain and spatial resolution. The observed development of upwelling occurs both due to a decrease in the surface temperature of the water, which cannot be lower than the temperature of deep waters, and due to the expansion of the area of cold surface waters.

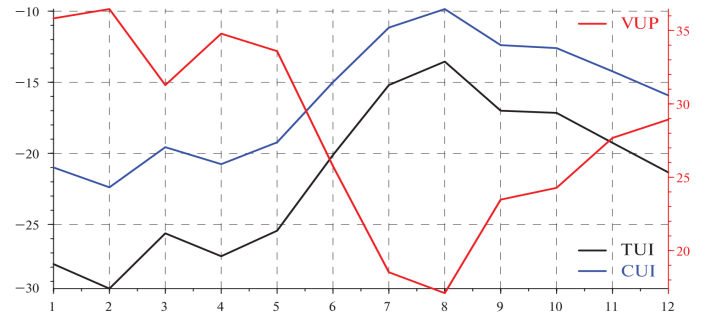


Fig. 3: The monthly average values of TUI (black line), CUI (blue line) and VUP (red line and scale) for the period 1985-2017, calculated inside monthly climate masks

When calculating the climatic TUI for each monthly mask, it should be taken into account that the area, and hence the number of points in the masks, will be different. For the correct calculation, the total temperature inside the mask must be divided by a constant value, which in this case will be equal to the number of points in the maximum mask. Calculations of the average values of any other parameters (wind speed, sea level, etc.) must be carried out inside the maximum mask area selected from 12 climate masks. In fig. Figure 3 shows the changes in the monthly climatic values of TUI, CUI and VUP for the entire Canary Upwelling region (the maximum water rise was in February and the minimum in August). The upwelling intensity is characterized not only by the thermal upwelling index, which reflects the contrast of the ocean surface temperature between coastal upwelling waters and the waters of the open ocean, but also by the Ekman transport value, which depends on the tangential wind friction, the type of coastline, and the Coriolis parameter. This characteristic is called the Ekman upwelling index (EUI). EUI is calculated from the Ekman transport (Q), which is created by the shear stress of wind friction [7], [26], [27], according to the formula:

$$EUI = -Q_x \cdot \sin(\phi) + Q_y \cdot \cos(\phi) \quad (3)$$

where Q_x and Q_y are the zonal and meridional components of the Ekman transport; ϕ is the angle of inclination of the coastline to the horizontal. The coastline of part of the northwestern coast of Africa (Canary Upwelling) was approximated by three straight sections with tilt angles of 135, 90, and 50. A positive EUI creates favorable conditions for upwelling, a negative value for downwelling. In addition to the Ekman transport considered above, by which the EUI was built, wind upwelling can also develop due to the Ekman pumping, associated with the positive vorticity of the wind friction stress field. Ekman pumping leads to divergence of the water surface, thereby increasing the vertical component of the current velocity, which leads to increased upwelling. The Ekman pumping speed W_E (the rate of water rise at a positive value) can be calculated from the components of the Ekman transport using the following formula:

$$W_E = \frac{\partial Q_x}{\partial x} + \frac{\partial Q_y}{\partial y} \quad (4)$$

The positive vorticity of the wind friction stress on the sea surface causes divergence and, accordingly, upwelling. Compared to Ekman transport, Ekman pumping makes the same or even greater contribution to upwelling processes in many regions (Taufikurrahman, Hidayat, 2017). In fig. Figure 4 shows the climatic values of EUI, W_E , and VUP calculated within the monthly climate masks. Values of W_E (or ekman pumping, EP) lie in the range $(-3.4...11.27) \times 10^{-7} m/s$. EUI values are calculated from the effective Ekman wind and occupy the range $(0.22... 0.94) m^2/s$. VUP values are in the range $(1.71 - 3.65) 10^6 C^2 km^2$. For all three graphs, general patterns can be distinguished that show increased upwelling in the winter-spring period and a weakening in the summer.

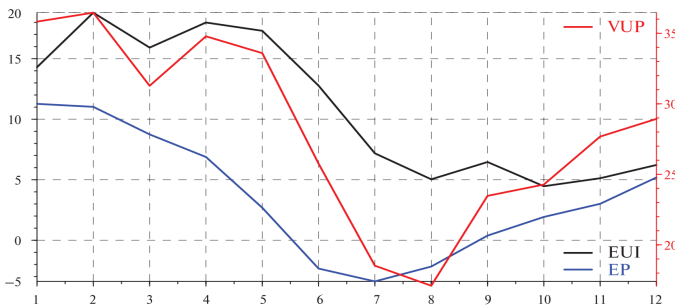


Fig. 4: Monthly average values of the Ekman upwelling index EUI (black line), Ekman pumping speed W_E (blue EP line and scale) and apparent upwelling power VUP (red line) for the period 1985-2017 calculated within the monthly climate masks

IV. CONCLUSION

Using the Canary Upwelling as an example, an improved technique for determining coastal upwelling indices is considered. Using this technique, the average values of the upwelling indices and any other parameters related to upwelling (water surface temperature, surface wind speed, sea level, geostrophic current, etc.) are determined inside the monthly

climate masks. The improved technique allows you to more accurately calculate the upwelling limits in each climate month and more accurately calculate its indices and other parameters. One of the most important characteristics of coastal wind upwelling is the area of its waters. The observed increase in upwelling occurs due to the temperature and volume of the raised colder deep waters, which on the sea surface create a temperature contrast between upwelling and surrounding waters. To account for the area of upwelling waters, modifications of the thermal upwelling index were proposed: cumulative index and apparent power. These indices take into account the temperature and the area of each upwelling point, and for VUP, the temperature is squared for a more significant separation of deep waters from distilled waters. The offshore zone used to calculate TUI and its modifications (CUI, VUP) was taken equidistant from the coastline (see Fig. 2). When calculating the boundaries of the upwelling waters from which the climate masks were built, we used the fact that the climatic SST graph has an inflection point at a certain longitude (see Fig. 1), starting from which the water temperature decreases more sharply when approaching the coast.

REFERENCES

- [1] Franklin B Schwing, Michael O'Farrell, John M Steger, and Kenneth Baltz, "Coastal upwelling indices west coast of north america," *NOAA Tech. Rep., NMFS SWFSC NMFS SWFSC*, vol. 231, pp. 144p, 1996.
- [2] Jonathan Roughgarden, Steven Gaines, and Hugh Possingham, "Recruitment dynamics in complex life cycles," *Proc. Natl. Acad. Sci. USA*, vol. 85, pp. 7418, 1988.
- [3] Anass El Aouni, Khalid Minaoui, Ayoub Tamim, Khalid Daoudi, Hussein Yahia, Abderrahman Atillah, and Driss Aboutajdine, "Detection of moroccan coastal upwelling using sea surface chlorophyll concentration," in *2015 IEEE/ACS 12th International Conference of Computer Systems and Applications (AICCSA)*. IEEE, 2015, pp. 1-4.
- [4] Fátima M Sousa, Susana Nascimento, Hugo Casimiro, and Dmitri Boutov, "Identification of upwelling areas on sea surface temperature images using fuzzy clustering," *Remote Sensing of Environment*, vol. 112, no. 6, pp. 2817-2823, 2008.
- [5] Andrew Bakun, "Daily and weekly upwelling indices, west coast of north america," *NOAA Tech. Rpt.*, vol. 16, 1975.
- [6] Anass El Aouni, Véronique Garçon, Joël Sudre, Hussein Yahia, Khalid Daoudi, and Khalid Minaoui, "Physical and biological satellite observations of the northwest african upwelling: Spatial extent and dynamics," *IEEE Transactions on Geoscience and Remote Sensing*, 2019.
- [7] Mark H Pickett and Jeffrey D Paduan, "Ekman transport and pumping in the california current based on the us navy's high-resolution atmospheric model (coamps)," *Journal of Geophysical Research: Oceans*, vol. 108, no. C10, 2003.
- [8] Anass El Aouni, Khalid Minaoui, Ayoub Tamim, Khalid Daoudi, and Hussein Yahia, "An improved method for accurate computation of coastal upwelling index using sea surface temperature images," in *2018 9th International Symposium on Signal, Image, Video and Communications (ISIVC)*. IEEE, 2018, pp. 76-81.
- [9] Anass El Aouni, Khalid Daoudi, Hussein Yahia, Khalid Minaoui, and Aïssa Benazzouz, "Surface mixing and biological activity in the north-west african upwelling," *Chaos: An Interdisciplinary Journal of Nonlinear Science*, vol. 29, no. 1, pp. 011104, 2019.
- [10] Vincent Rossi, Cristóbal Lopez, Emilio Hernández-García, Joel Sudre, Véronique Garçon, and Yves Morel, "Surface mixing and biological activity in the four eastern boundary upwelling systems," *arXiv preprint arXiv:0909.0115*, 2009.
- [11] Vincent Rossi, Cristóbal López, Joel Sudre, Emilio Hernández-García, and Véronique Garçon, "Comparative study of mixing and biological activity of the benguela and canary upwelling systems," *Geophysical Research Letters*, vol. 35, no. 11, 2008.
- [12] Francesco d'Ovidio, Vicente Fernández, Emilio Hernández-García, and Cristóbal López, "Mixing structures in the mediterranean sea from finite-size lyapunov exponents," *Geophysical Research Letters*, vol. 31, no. 17, 2004.

- [13] Anass El Aouni, Khalid Daoudi, Hussein Yahia, and Khalid Minaoui, "Surface mixing and biological activity in the north african upwelling," 2018.
- [14] Timothy J Osborn, "Winter 2009/2010 temperatures and a record-breaking north atlantic oscillation index," *Weather*, vol. 66, no. 1, pp. 19–21, 2011.
- [15] Hervé DEMARCQ and Valérie FAURE, "Coastal upwelling and associated retention indices derived from satellite sst. application to octopus vulgaris recruitment," *Oceanologica Acta*, vol. 23, no. 4, pp. 391–408, 2000.
- [16] Anass El Aouni, Khalid Daoudi, Hussein Yahia, and Khalid Minaoui, "The contribution and influence of coherent mesoscale eddies off the north-west african upwelling on the open ocean," 2019.
- [17] L Jiang, LC Breaker, and X-H Yan, "A model for estimating cross-shore surface transport with application to the new jersey shelf," *Journal of Geophysical Research: Oceans*, vol. 115, no. C4, 2010.
- [18] Judah Cohen, James Foster, Mathew Barlow, Kazuyuki Saito, and Justin Jones, "Winter 2009–2010: A case study of an extreme arctic oscillation event," *Geophysical Research Letters*, vol. 37, no. 17, 2010.
- [19] Susana Nascimento, Pedro Franco, Fátima Sousa, Joaquim Dias, and Filipe Neves, "Automated computational delimitation of sst upwelling areas using fuzzy clustering," *Computers & Geosciences*, vol. 43, pp. 207–216, 2012.
- [20] Theo Pavlidis and Yuh-Tay Liow, "Integrating region growing and edge detection," *Pattern Analysis and Machine Intelligence, IEEE Transactions on*, vol. 12, no. 3, pp. 225–233, 1990.
- [21] Kenneth H Mann and John RN Lazier, *Dynamics of marine ecosystems: biological-physical interactions in the oceans*, John Wiley & Sons, 2013.
- [22] L Van Camp, L Nykjaer, E Mittelstaedt, and P Schlittenhardt, "Upwelling and boundary circulation off northwest africa as depicted by infrared and visible satellite observations," *Progress in Oceanography*, vol. 26, no. 4, pp. 357–402, 1991.
- [23] Anass El Aouni, Khalid Minaoui, Khalid Daoudi, and Hussein Yahia, "North-west african upwelling dynamics from physical and biological satellite observations," 2018.
- [24] Philippe Cury and Claude Roy, "Optimal environmental window and pelagic fish recruitment success in upwelling areas," *Canadian Journal of Fisheries and Aquatic Sciences*, vol. 46, no. 4, pp. 670–680, 1989.
- [25] A Miguel P Santos, Alexander S Kazmin, and Alvaro Peliz, "Decadal changes in the canary upwelling system as revealed by satellite observations: their impact on productivity," *Journal of Marine Research*, vol. 63, no. 2, pp. 359–379, 2005.
- [26] ST Gille, MM Carranza, R Cambra, and R Morrow, "Wind-induced upwelling in the kerguelen plateau region," *Biogeosciences*, vol. 11, no. 22, pp. 6389–6400, 2014.
- [27] V Walfrid Ekman, "On the influence of the earth's rotation on ocean currents," *Ark. Mat. Astron. Fys.*, vol. 2, pp. 1–53, 1905.